Innovative aerosol hygroscopic growth study from Mie-Raman-Fluorescence lidar and Microwave Radiometer synergy

Robin Miri[1], Olivier Pujol[1], Qiaoyun Hu[1], Philippe Goloub[1], Igor Veselovskii[2,3], Thierry Podvin[1], Fabrice Ducos[1]

[1]Univ. Lille, CNRS, UMR 8518 – LOA – Laboratoire d'Optique Atmosphérique, Villeneuve d'Ascq 59650, France
[2]Prokhorov General Physics Institute of the Russian Academy of Sciences, Moscow, Russia
[3]Cimel Electronique, 172 rue de Charonne 75011 Paris, France

Correspondence to: Robin Miri (robin.miri@univ-lille.fr)

Abstract. This study focuses on the characterization of aerosol hygroscopicity using remote sensing techniques. We employ a Mie-Raman-Fluorescence lidar (LILAS), developed at the ATOLL platform, Laboratoire d'Optique Atmosphérique, Lille, France, in combination with the RPG-HATPRO G5 microwave radiometer to enable continuous aerosol and water vapor monitoring. We identify hygroscopic growth cases when an aerosol layer exhibits an increase in both aerosol backscattering coefficient and relative humidity. By examining the fluorescence backscattering coefficient, which remains unaffected by the presence of water vapor, the potential temperature and the absolute humidity, we verify the homogeneity of the aerosol layer. Consequently, the change in the backscattering coefficient is solely attributed to water uptake. The Hänel theory is employed to describe the evolution of the backscattering coefficient with relative humidity and introduces a hygroscopic coefficient, γ, which depends on the aerosol type. The particularity of this method revolves in the use of the fluorescence which is employed to take into account and correct the aerosol concentration variations in the layer. Case studies conducted on 29 July and 9 March, 2021 examine respectively an urban and a smoke aerosol layer. For the urban case, γ is estimated as 0.47±0.03 at 532 nm; as for the smoke case, the estimation of γ is 0.5±0.3. These values align with those reported in the literature for urban and smoke particles. Our findings highlight the efficiency of the Mie-Raman-Fluorescence lidar and Microwave radiometer synergy in characterizing aerosol hygroscopicity. The results contribute to advance our understanding of atmospheric processes, aerosol-cloud interactions, and climate modeling.

Key words:

Aerosols, Hygroscopicity, Fluorescence Lidar, Microwave Radiometer

1 Introduction

Aerosols play a crucial role in our understanding of climate dynamics. Their impact on the radiation budget is classified into direct and semi-direct effects (Hansen et al., 1997; Thorsen et al., 2020), with additional contributions arising from aerosol-

cloud interactions, commonly known as indirect effects. Certain aerosols can act as cloud condensation nuclei (CCN) or ice

30 nucleating particle (INP), altering cloud properties including albedo and lifetime (Twomey et al., 1967). These complex processes remain significant challenges in the interpretation of the Earth energy balance. To advance our comprehension of aerosol-cloud interactions is crucial for improving climate models and accurately accounting for their influence on the energy balance of our planet. A key process in the understanding of these interactions is hygroscopic growth, which consists in aerosol uptake of water vapor in high relative humidity (RH) conditions, resulting in changes in size and, in some cases, chemical

35 composition (Hänel, 1976). Hygroscopic growth efficiency varies depending on the aerosol type, with hydrophobic aerosols like dust and hydrophilic aerosols like marine particles (Chen et al., 2019; Chen et al., 2020). This variability is linked to their potential as CCN and INP, highlighting the importance of understanding the hygroscopic properties of aerosols (Dusek et al., 2006).

Hygroscopic growth properties of aerosols can be effectively investigated using a range of instruments. Traditionally,

40 humidified nephelometers and spectrometers have been widely used to study aerosol hygroscopicity (Covert et al., 1972; Burgos et al., 2019). However, active remote sensing systems tend appear more advantageous since the last decade as they allow to measure with high vertical and temporal resolution, without interfering with the observed system. Lidars, in particular, have gained prominence in remotely studying these properties (Feingold and Morley, 2003; Fernández et al., 2015; Granados-Muñoz et al., 2015; Zieger et al., 2015; Navas-Guzmán et al., 2019; Dawson et al., 2020; Düsing et al., 2021; Sicard et al.

45 2022…) and offer several advantages compared to other methods. In particular, lidars provide high vertical and temporal resolution, allowing for detailed analysis of aerosol characteristics. Moreover, lidars offer the unique capability of simultaneously measuring aerosol properties and water vapor mixing ratio using a single instrument. At the Laboratoire d'Optique Atmosphérique (LOA) in Lille, France, the ATOLL platform (ATmospheric Observations at LiLLe) features a Mie-Raman-Fluorescence lidar (Lille Lidar for Atmospheric Study, LILAS) employed in the frame of EARLINET/ACTRIS-FR

50 (European Aerosol Research Lidar Network/Aerosols, Clouds and Trace Gases Research Infrastructure-France). This multiwavelength lidar system measures elastic, depolarized and Raman signals, providing comprehensive information on aerosol properties and water vapor. Additionally, LILAS captures aerosol fluorescence signal at 466 nm, which is triggered by the lidar UV wavelength at 355 nm. The fluorescence signal possesses distinctive characteristics that contribute to its utility in aerosol studies. Its intensity correlates with aerosol concentration and type, with biological aerosols like pollen or biomass

55 burning smoke exhibiting higher fluorescence, while pure dust or urban aerosols demonstrate lower fluorescence. Furthermore, the fluorescence signal at 466 nm does not arise from pure water, enabling the extraction of aerosol-specific information without the influence of water vapor, which proves to be essential in studying aerosol hygroscopic growth (Veselovskii et al., 2020). In combination with an RPG-HATPRO G5 microwave radiometer, also part of the ATOLL platform, it is possible to monitor both aerosol characteristics and water vapor, allowing to study aerosol hygroscopicity.

60 The first part of this paper introduces the instruments, and outlines a novel method for the study of aerosol hygroscopic growth using LILAS measurements. Following the instrument and method description, case studies are presented to demonstrate the efficiency and potential of the proposed approach. These case studies illustrate the practical implementation and feasibility of

this innovative methodology, highlighting the added value brought by aerosol fluorescence measurement in offering valuable insights into the hygroscopic growth characteristics of these aerosols. Finally, the paper concludes with a summary of the findings and offers comments on the obtained results. The conclusions will also discuss the potential further advancements and applications of the developed method, emphasizing its importance in enhancing our understanding of hygroscopic growth phenomena and its broader implications for atmospheric research.

2 Instrumentation and methodology

2.1 Experimental setup and data treatment

All the measurements presented in this paper were performed at the ATOLL platform in Lille (50.611° N, 3.138° E). The first instrument used in this study is the lidar LILAS. Its emission component consists of a tripled Nd:YAG laser operating at a repetition rate of 20 Hz, with a pulse energy of 70 mJ at 355 nm. The lidar system is configured in the $3\beta + 2\alpha + 3\delta$ arrangement, meaning it measures the elastic backscatter coefficient at three wavelengths (355 nm, 532 nm and 1064 nm), it also measures the extinction at 355 nm and 532 nm, as well as the volume depolarization ratios for these wavelengths. This instrument also includes an additional channel for aerosol fluorescence detection, featuring a dedicated interference filter centred at 466 nm with a width of 44 nm. For this study, the aerosol elastic backscatter coefficients (β) and the particulate linear depolarization ratio (PLDR) were computed at 532 nm from Mie-Raman observation (Ansmann et al., 1992) due to the high signal to noise ratio at this wavelength in comparison with the two others. Furthermore, the detection part of the lidar includes a channel specifically designed to measure the vibrational-rotational Raman scattering of water at 408 nm, allowing for the retrieval of water vapor mixing ratio profiles (Ansmann et al., 1992, Whiteman et al. 1992). The obtained profiles were acquired during night time only, and averaged over a period of 60 minutes. General details about the system can be found in Hu et al. (2018) and Veselovskii et al. (2020).

The proximity of the ATOLL platform to the airport prohibits the use of radiosounding. This poses a challenge for the inversion of water vapor using the LILAS lidar, as the computation of the instrumental constant requires a reference. Moreover, radiosoundings traditionally provide temperature profiles, which are crucial for calculating RH but are difficult to obtain otherwise.

The second instrument used in this study is the RPG-HATPRO G5 microwave radiometer developed by Radiometer Physics present at the ATOLL platform which provides integrated information like Integrated Water Vapor content (IWV) or Liquide Water Content (LWC), but also uses an integrated neural network model to retrieve atmospheric profiles of temperature, humidity, and liquid water. In situ sensors allow for ground level measurement of temperature, humidity and pressure. Finally, an infrared radiometer extension allows to detect cloud base height and ice clouds. Data are acquired at high temporal resolution (every 10 minutes) and profiles range from the ground to 10km (Louf et al., 2015).

This instrument has been considered to compensate for the lack of radiosounding measurement at the ATOLL platform for the calibration of the lidar water vapor measurement. Unfortunately, after considering using the radiometer humidity and
95   temperature profiles for the lidar calibration, these ones turned out to be insufficiently accurate.

Consequently, temperature profiles from the ERA-5 reanalysis database were also collected, and the IWV measurement of the radiometer has been used to calibrate the lidar.

In order to compute the instrumental constant necessary for the lidar water vapor calibration, the radiometer IWV has been compared to the integral of absolute humidity (AH) between the ground and 6 km (above which humidity is negligible), derived
100   from the lidar-measured water vapor mixing ratio and the ERA-5 temperature. Following the calibration procedure described in Foth et al. (2015), the calibration constant of the instrument is determined as the ratio between IWV and the integral value. The calibrated water vapor mixing ratio can be computed with:

$$x_{H_2O}(h) = x'_{H_2O}(h) IWV \left[\int_0^{z_{max}} x'_{H_2O}(h) \frac{P(h)}{R_a T(h)} dh \right]^{-1} , \qquad (1)$$

where h is the height, $x_{H_2O}(h)$ and $x'_{H_2O}(h)$ the calibrated and not-calibrated water vapor mixing ratios respectively, z_{max} is
105   equal to 6 km, P is the atmospheric pressure estimated with the hydrostatic approximation, R_a is the air perfect gas constant, T is the temperature all given in the International System of units. The calibration has been exclusively conducted under clear sky conditions and taking into account the signal-to-noise ratio of the lidar's water vapor mixing ratio: if the signal to noise ratio on the profile is lower than 3, the calibration constant is not computed. This threshold has been determined to ensure both data quality and a sufficient number of calibration constant computations. An interpolation has then been performed to estimate
110   the calibration constants of cloudy and noisy situations.

2.2 Hygroscopic growth identification & study

In order to identify and analyze hygroscopic growth cases, a widely used method consists in searching for a homogeneous aerosol layer that spans either in time or altitude. When RH and elastic backscatter coefficient both increase, or decrease, it serves as a key indicator of hygroscopic growth. In the case of a homogeneous aerosol layer, the elastic backscatter coefficient
115   evolution can then be attributed only to hygroscopic growth. This approach enables to relate the elastic backscatter coefficient and RH, characterizing the hygroscopic properties of the considered aerosol particles.

The verification of the homogeneous nature of the considered aerosol layer is generally performed by investigating two key variables, absolute humidity and potential temperature. Absolute humidity is investigated in order to identify any changes in the air mass, that would lead to a change in the absolute humidity. A constant or decreasing potential temperature means that
120   strong mixing is occurring within the layer, thus supporting that the layer is homogeneous (Granados-Muñoz et al., 2015; Navas-Guzmán et al., 2019; Sicard et al. 2022).

The focus of this paper rounds about the valuable insights provided by β_{fluo}. As stated in Veselovskii et al. (2020), fluorescence signal emitted by aerosols around 466 nm is not expected to be impacted by the presence of water, as pure water does not fluoresce. Therefore, by assuming that hygroscopic growth does not impact aerosol fluorescence and that the aerosol mixing

state remains the same in the considered layer, β_{fluo} becomes a reliable proxy for monitoring the concentration of dry material within the aerosol layer. Under the hypothesis of a constant aerosol mixture and chemical composition in the layer, normalizing β_{532} by β_{fluo} enables the study of hygroscopic growth properties, while also accounting for any possible changes in aerosol concentration within the layer.

Once the hygroscopic growth case has been identified, it becomes possible to examine the correlations between aerosol optical properties and RH. In this paper, particular attention has been given in the investigation of β_{532}. In order to explore this correlation efficiently, the Hänel parametrization has been used to express the changes in β_{532} as a function of RH. It introduces a parameter γ, known as the hygroscopic growth factor, which depends on the wavelength and the type of aerosol (Hänel, 1976). The Hänel parametrization is represented by:

$$\frac{\beta_{532}(RH)}{\beta_{532}(RH_{ref})} = \left(\frac{100-RH}{100-RH_{ref}}\right)^{-\gamma}, \tag{2}$$

RH_{ref} being the reference relative humidity. From this parametrization, it is possible to use β_{fluo} to account for aerosol concentration changes within the layer, by normalizing β_{532} such as:

$$\frac{\beta_{532}(RH)}{\beta_{532}(RH_{ref})}\frac{\beta_{fluo}(RH_{ref})}{\beta_{fluo}(RH)} = \left(\frac{100-RH}{100-RH_{ref}}\right)^{-\gamma}, \tag{3}$$

We obtain an accurate estimation of the hygroscopic parameter γ, by fitting the variation of β_{532} with respect to RH to the function:

$$\beta_{532}(RH) = \beta_{532}(RH_{min})\frac{\beta_{fluo}(RH)}{\beta_{fluo}(RH_{min})}\left(\frac{100-RH}{100-RH_{min}}\right)^{-\gamma}, \tag{4}$$

where RH_{min} represents the minimum relative humidity observed within the analysed aerosol layer. Subsequently, the estimations of γ values can be compared to hygroscopic growth parameter estimations from previous studies, the type of the aerosol can be estimated from the optical properties, mainly its fluorescence capacity (the ratio between the fluorescence and elastic backscatter coefficients) and PLDR (Veselovskii et al, 2022) as shown Figure 1. This comparative analysis offers valuable insights on how the hygroscopic growth of aerosols relates to their specific compositions and sources, contributing to a deeper understanding of aerosol behaviour in changing environmental conditions.
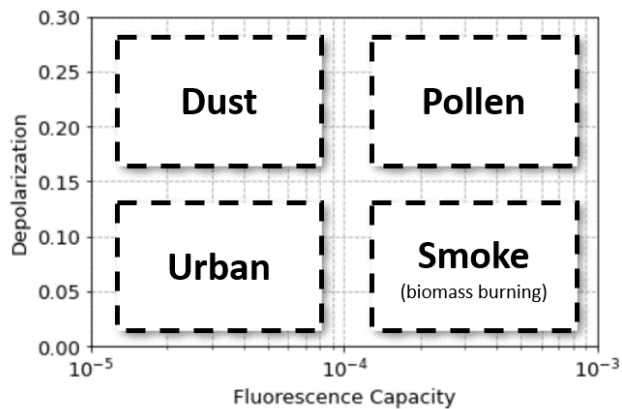
Figure 1: Schematic empirical aerosol typing repartition in function of the Depolarization (PLDR) & Fluorescence capacity (adapted from Veselovskii et al. 2022)

150   3 Results and discussions

In order to experiment the potential of the hygroscopic growth study approach, this method has been tested on two potential hygroscopic growth cases, the first one occurring during 29 July 2021, averaged from 22:00 to 23:00 UTC, and the second during 9 March 2021, averaged from 21:00 to 22:00 UTC.

3.1 Hygroscopic growth study during the event of 29 July 2021, from 22:00 to 23:00 UTC
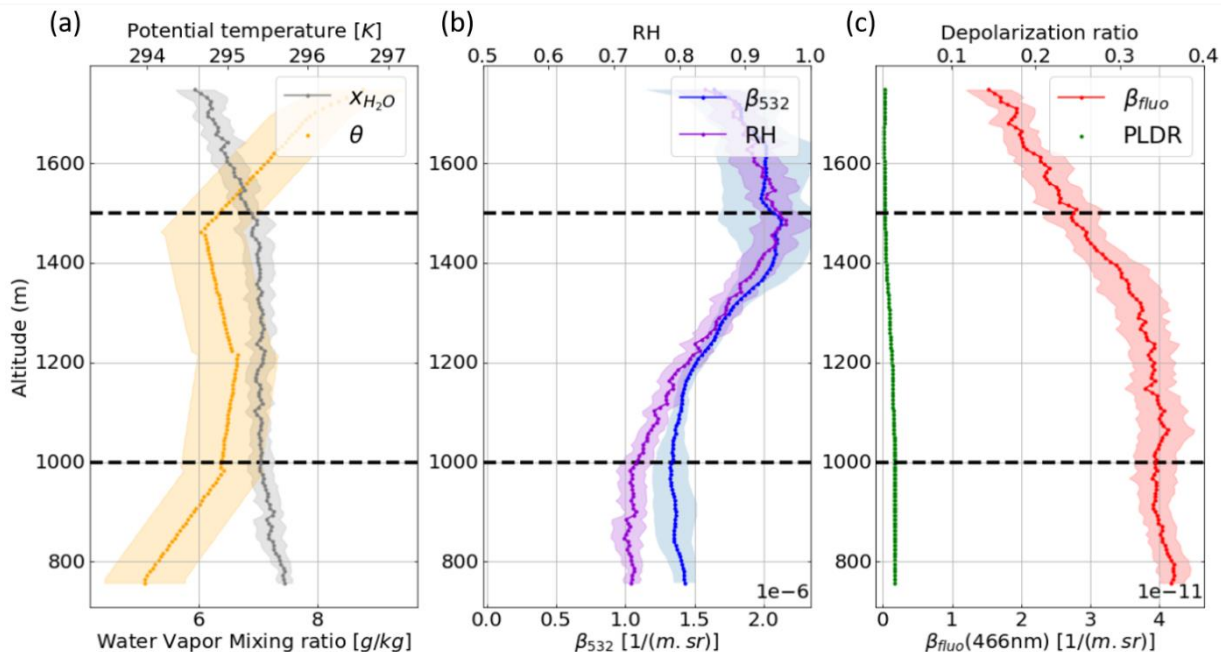
155

Figure 2: Profile of retrieved optical properties in function of altitude above ground level (a) water vapor mixing ratio [g/kg] and potential temperature [K], (b) elastic backscatter coefficient at 532 nm [1/m.sr] and RH, (c) fluorescence backscatter coefficient at 466 nm [1/m.sr] and particular linear depolarization ratio at 532 nm, on 29 July 2021 from 22:00 to 23:00 UTC, the black dashed lines identify the area where hygroscopic growth is expected to occur

160 Figure 2 shows the profiles of the different measurements on the case study of 29 July 2021. In this particular scenario, both the water vapor mixing ratio and potential temperature exhibit relative stability, which are the two criteria commonly used to assess that the considered aerosol layer is homogeneous (Granados-Muñoz et al., 2015; Navas-Guzmán et al., 2019; Sicard et al., 2022). Even though the potential temperature is derived from ERA-5 reanalysis temperature profiles rather than direct measurements, this still provides a strong indication of the aerosol layer homogeneity. Moreover, β_{fluo} does not show strong

165 variations within the defined region (the standard deviation of β_{fluo} in the considered layer is about 10% of the average), further supporting this conclusion.

Conversely, there is an increase in both β_{532} and RH, suggesting a potential case of hygroscopic growth. RH rises from 74% to 96% which is a significant growth and strongly support the hypothesis that hygroscopic growth occurs. Lastly, the PLDR slightly decreases, but given its already low value, further decrease due to hygroscopic growth is not anticipated.

170 Finally, it is possible to estimate the aerosol type of the considered layer by looking at its optical properties. Figure 3 shows the scatter plot of the PLDR at 532 nm and the fluorescence capacity which is here the ratio between β_{fluo} and β_{532}. The considered aerosol layer exhibits low PLDR as well as low fluorescence capacity, characteristics that allow it to be identified as an urban aerosol layer.
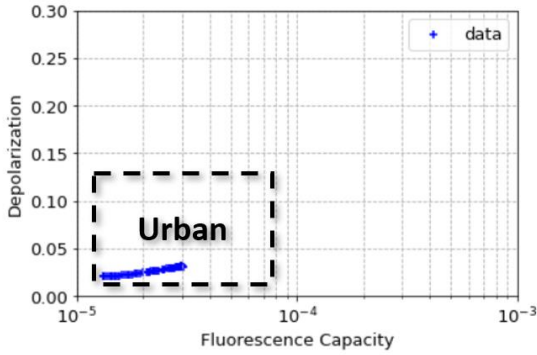
175 **Figure 3: Fluorescence capacity (β_{fluo}/β_{532}) and Particle Linear Depolarization Ratio at 532 nm between 1000 m and 1500 m above ground level on 29 July 2021 from 22:00 to 23:00 UTC, characteristic of an urban aerosol layer.**
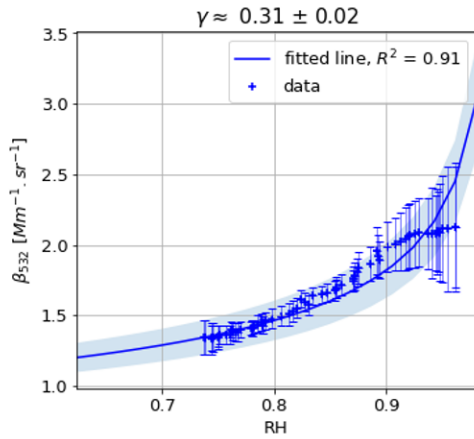
Figure 4: Evolution of the elastic backscatter coefficient at 532 nm in function of RH on 29 July 2021 from 22:00 to 23:00 UTC, between 1000 m and 1500 m above ground level, and results of the fit on the Hänel parametrization

180 Figure 4 presents the outcomes of the fitting process for the relationship between β_{532} and RH using the Hänel parametrization. These results indicate a good fit to the Hänel parametrization in this particular case, as evidenced by the determination coefficient being close to 1 ($R^2 = 0.91$). However, the estimated value of γ, which is expected to fall between 0.3 and 0.5 for a case of urban particles (Navas-Guzmán et al., 2019), is equal to 0.31 in this instance, which is very close to the lower limit for this type of aerosols. It also comes along with a slight divergence between the fit and the data, specially at high RH.

185 Several factors may contribute to the deterioration of the results and explain the low value of γ. First, it is possible that in this case, there is merely no significant hygroscopic growth occurring for this particular type of aerosol within the observed range of RH. However, given the substantial RH variation, starting at 74% and reaching up to 96%, this hypothesis becomes less plausible.

Second, it is possible that the main assumption on which lies this parametrization, i.e. constant aerosol concentration within

190 the observed layer, may not hold true. Even with stable potential temperature and water vapor mixing ratio, there is a possibility that aerosol concentration varies within the designated area, especially considering that potential temperature is derived from

ERA-5 reanalysis profiles and not directly measured. This potential aerosol concentration variation could potentially account for the low estimation of the hygroscopic growth factor.

In order to investigate this, we can assume that aerosol mixing remains constant within the study area, and that β_{fluo} varies
195 solely with changes in aerosol concentration. Doing so, it becomes possible to normalize β_{532} based on variations in aerosol concentration according to:

$$\overline{\beta_{532}}(RH) = \beta_{532}(RH)\frac{\beta_{fluo}(RH_{min})}{\beta_{fluo}(RH)}, \tag{4}$$

Here, $\overline{\beta_{532}}(RH)$ is the normalized elastic backscatter coefficient and $\beta_{fluo}(RH_{min})$ is β_{fluo} at the minimum value of RH in the studied area.

200 It is now possible to apply the Hänel parametrization on $\overline{\beta_{532}}$ instead of β_{532} to take into account aerosol concentration variations within the layer, and assess whether this normalization yields improved results.
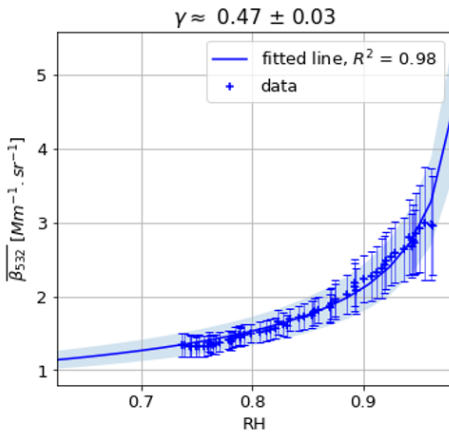
Figure 5: Evolution of the normalized elastic backscatter coefficient at 532 nm (normalized with fluorescence backscatter coefficient) in function of RH on 29 July 2021 from 22:00 to 23:00 UTC, between 1000 m and 1500 m above ground level, and results of the fit
205 **on the Hänel parametrization**

The relationship between $\overline{\beta_{532}}$ and RH, along with its fit to the Hänel parametrization presented in Figure 5 demonstrate a significantly improved fit to the Hänel parametrization, with a notably higher determination coefficient ($R^2 = 0.98$ instead of 0.91). Furthermore, the estimation of γ is found to be equal to 0.47 ± 0.03, falling precisely within the range of estimations conducted at 532 nm by previous studies (Navas-Guzmán et al. 2019, Sicard et al. 2022). These findings support the hypothesis
210 that aerosol concentration varies within the aerosol layer, and that such fluctuations are traceable through β_{fluo}, corroborating the efficiency of the presented approach for investigating hygroscopic growth phenomena.

3.2 Hygroscopic growth study during the event of 9 March, from 21:00 to 22:00 UTC

Another case study can be presented to further support the validity of this approach. It is the case occurring on 9 March 2021 averaged between 21:00 UTC and 22:00 UTC.
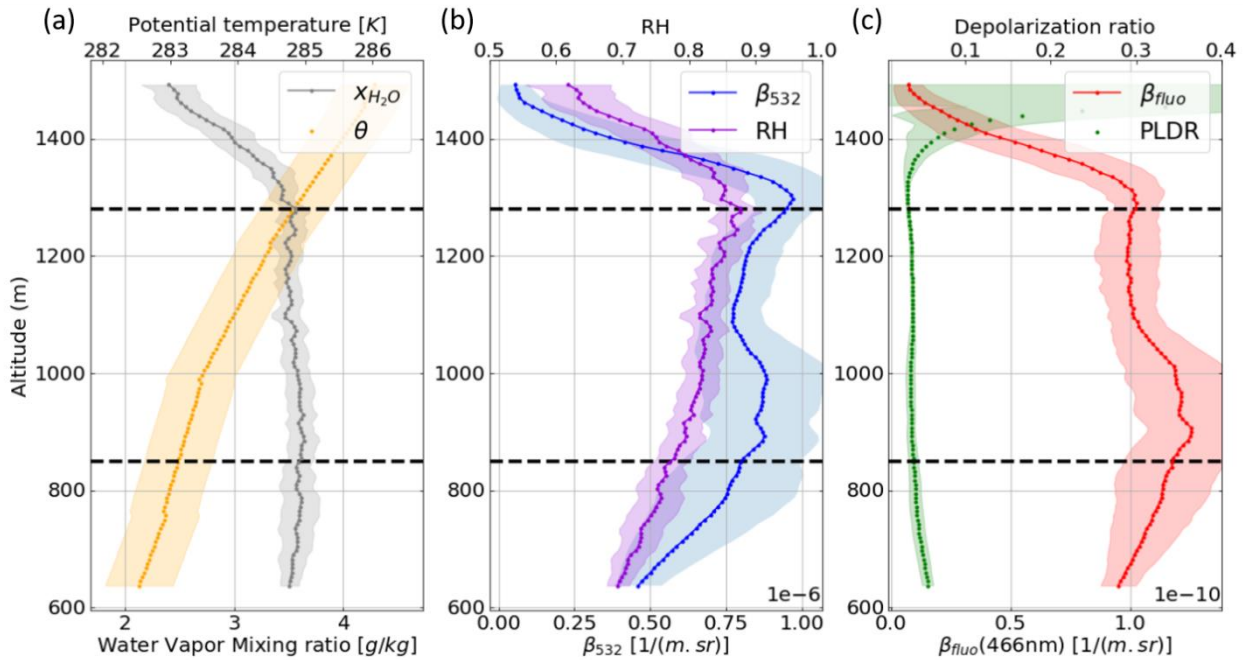
215

Figure 6: Profile of retrieved optical properties in function of altitude above ground level (a) water vapor mixing ratio [g/kg] and potential temperature [K], (b) elastic backscatter coefficient at 532 nm [1/m.sr] and relative humidity, (c) fluorescence backscatter coefficient at 466 nm [1/m.sr] and particular linear depolarization ratio at 532 nm, on 9 March 2021 from 21:00 to 22:00 UTC, the black dashed lines identify the area where hygroscopic growth is expected to occur

220 Figure 6 shows the profiles of the different measurements on the case study of 9 March 2021. In this situation, both the water vapor mixing ratio and the potential temperature are relatively stable in the layer (potential temperature variations remain under 2 K, and the water vapor mixing ratio variations remain under 1 g/kg), indicating a good mixing in the considered layer. An increase in both RH and β_{532} can also be noticed. On the other hand, there are fluctuations of β_{fluo}, mostly in the lower part of the layer, and the PLDR remains stable, but once again, given its already low value, it is not expected to decrease with

225 hygroscopic growth. These elements together indicate that a hygroscopic growth scenario is most likely to occur in this layer. The aerosol type can be investigating once again by looking at the fluorescence capacity and the PLDR. Both are represented Figure 7 and show characteristics indicating that the aerosol layer comes from biomass burning smoke with low PLDR and strong fluorescence. Something worth noticing however is the low value of the fluorescence capacity. Indeed, the fluorescence capacity is the ratio between fluorescence backscatter coefficient and elastic backscatter coefficient. While the first one is

230 expected to remain stable with hygroscopic growth, the second increases in high humidity condition, consequently decreasing the fluorescence capacity and potentially leading to misclassification as indicated in Veselovskii et al., 2020. In this case however, it is still possible to identify the biomass burning smoke aerosol layer.
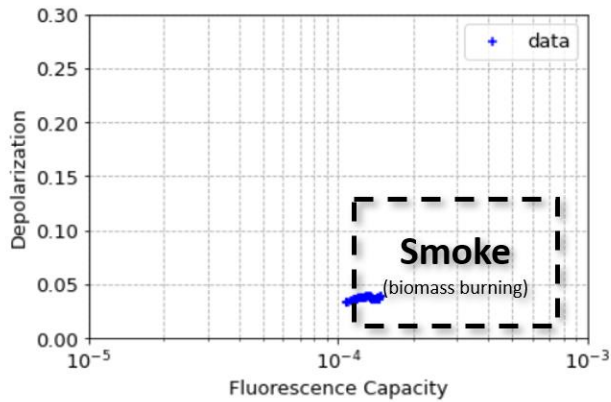
Figure 7: Fluorescence capacity (β_{fluo}/β_{532}) and Particle Linear Depolarization Ratio at 532 nm between 850 m and 1280 m above ground level on 9 March 2021 from 21:00 to 22:00 UTC, characteristic of a biomass burning smoke aerosol layer.
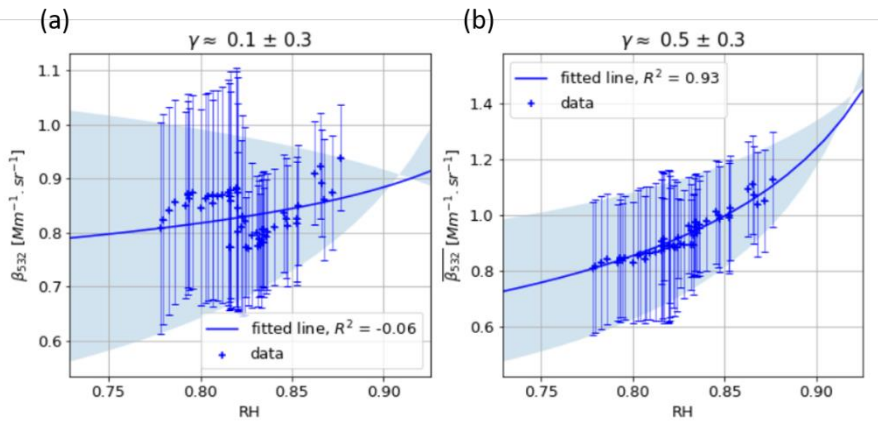
Figure 8: Evolution of the elastic backscatter coefficient at 532 nm (a) without normalization and (b) with normalization with the fluorescence backscatter coefficient, in function of RH on 9 March 2021 from 21:00 to 22:00 UTC, between 850 m and 1280 m above ground level, and results of the fit on the Hänel parametrization

The results of the fit to the Hänel parametrization on both β_{532} and $\overline{\beta_{532}}$ shown Figure 8 indicate a significant improvement brought by the normalization with the fluorescence. Without this process, the fit to the Hänel parametrization is extremely poor, with $R^2 = -0.06$. Furthermore, the estimation of the hygroscopic growth parameter is much lower than expected ($\gamma = 0.1 \pm 0.3$) while the value is expected to fall around 0.5 at 532 nm for smoke aerosols according to Gomez et al. (2018). On the other hand, by using the information given by the fluorescence to normalize the elastic backscatter coefficient, it is possible to obtain a much better fit to the Hänel parametrization, with $R^2 = 0.93$ and a better estimation of the hygroscopic growth parameter, with $\gamma = 0.5 \pm 0.3$ falling in the expected range for smoke aerosols. These findings suggest that it is indeed possible to use β_{fluo} to correct the variation of aerosol concentration within the aerosol layer to study hygroscopic growth. The only drawback of this case lays in its high uncertainty.

Explanation for this high uncertainty could be instrumental noise, or the span of RH covered being narrower than the first
250   presented case (RH varying from 77.8% to 87.6%), or even the atmospheric variability being more important in this situation. Nevertheless, the point demonstrated in this analysis relies in the utility of the fluorescence correction for the hygroscopic factor estimation which is well emphasized here.

The influence of a shift in RH on γ has also been examined. For the case of 9 March 2021, when a bias of minus 0.1 is manually introduced on RH, the corresponding γ estimation becomes 0.82, while a positive bias of 0.1 in RH results in a γ value of 0.23.
255   The estimation of RH is based on both measurement from LILAS and the radiometer but also on ERA-5 reanalysis data, which heavily relies on computational models. While this estimation provides valuable insights, it inherently introduces a level of uncertainty on the results. It is anticipated that the uncertainty associated with this estimation falls within the range of 10%. The estimation of γ and the conclusions draw from this estimation should then be considered with caution. Future studies might focus on refining the methods used for RH estimation, aiming at minimizing this inherent uncertainty and enhancing the
260   accuracy of these findings. However, even if a shift in RH introduces high variability in γ, the determination coefficient R^2 remains almost unchanged ($R^2 = 0.92$ when RH is decreased by 0.1 and $R^2 = 0.91$ for a 0.1 increase) meaning that the conclusion drawn on the use of the fluorescence correction are still valid in spite of the uncertainty on RH.

4. Conclusion

In this article, we have examined the possibility of using LILAS data for aerosol hygroscopic growth studies. The calibration
265   of LILAS's water vapor channel has been addressed using thermodynamic data from the RPG-HATPRO microwave radiometer and temperature data from ERA-5 reanalysis. A new approach to analyse aerosol hygroscopicity, relying on the fluorescence profiles measured by LILAS has been developed and tested on two situations.

The unique feature of the method presented in this article hinges on its use of the fluorescence backscatter coefficient. This coefficient serves as a weighting factor in tracking the evolution of aerosol concentration within the aerosol layer.
270   Consequently, it leads to a significantly improved representation of the hygroscopic state evolution of the aerosols, thereby enhancing the characterization of the Hänel hygroscopic coefficient, γ. To validate this approach, evaluations were performed on two cases from July and March 2021, yielding promising results and highlighting the value brought by the fluorescence backscatter coefficient measurement with the lidar. With, in the first case, an estimation of γ of 0.47 ± 0.03 with the fluorescence correction, falling in the expected range of hygroscopic growth parameter of urban aerosols at 532 nm. In the
275   second case, the estimation of γ is of 0.5 ± 0.3 which, despite higher uncertainty, is in the expected values for smoke particles at 532 nm and most importantly, is a great improvement compared to the estimation carried on without the fluorescence correction.

In order to further increase the accuracy of our results, this method could be applied on a site featuring both fluorescence lidar measurement as well as radiosoundings in order to better estimate RH, a variable that significantly influences γ estimation and
280   which is really complicated to estimate accurately otherwise. Based on the presented approach, values of γ can be calculated

for various types of aerosols, and the assessment of the relationship between γ and aerosol optical properties like PLDR or fluorescence capacity can be considered. These relationships are expected to provide valuable insights for modelling interactions between aerosols and water vapor, serving as an initial step in studying aerosol-cloud interactions (Dusek et al., 2006, Petters and Kreideweis, 2007).

285 However, a current limitation of the present work arises in the identification of hygroscopic growth cases which is made manually. Future efforts could focus on automatically identifying hygroscopic growth cases using lidar measurements, simplifying the study of γ dependency with aerosol parameters on a large number of situations (Gysel et al., 2007). In this perspective, an automatic classification method is also currently being developed using clustering approach in order to automatically classify aerosol layers based on their optical properties as well as thermodynamic parameters accounting for

290 humidity impact on the fluorescence capacity as illustrated in the analysis of Figure 7.

Furthermore, the hygroscopic growth study will be adapted and improved for the LIFE lidar (Laser Induced Fluorescence Explorer), anticipated to be operational by 2024. This upcoming lidar system is set to have more power and include additional fluorescence channels, thereby increasing the amount of information available, which will significantly enhance the retrieval performance.

295 **Code and data availability**

Data and code will be available upon the request

Competing interests

The contact author has declared that none of the authors has any competing interests.

Acknowledgements

300 We acknowledge CaPPA project funded by the ANR through the PIA under contract ANR-11-LABX-0005-01. The authors thank the Région Hauts-de-France, the Ministère de l'Enseignement Supérieur et de la Recherche and the European Fund for Regional Economic Development for their financial support to the CPER CLIMIBIO and ECRIN programs. The contribution from Q. Hu was supported by Agence Nationale de Recherche ANR (ANR-21-ESRE-0013) through the OBS4CLIM project. ChatGPT has been employed for the drafting purposes in this document.

305 **References**

Ansmann, A., Riebesell, M., Wandinger, U. *et al.* Combined raman elastic-backscatter LIDAR for vertical profiling of moisture, aerosol extinction, backscatter, and LIDAR ratio. *Appl. Phys. B* **55**, 18–28 (1992). https://doi.org/10.1007/BF00348608

Burgos, M.A., Andrews, E., Titos, G. et al. A global view on the effect of water uptake on aerosol particle light scattering. Sci
310   Data 6, 157 (2019). https://doi.org/10.1038/s41597-019-0158-7

Chen, Jun, Zhanqing Li, Min Lv, Yuying Wang, Wei Wang, Yingjie Zhang, Haofei Wang, Xing Yan, Yele Sun, and Maureen Cribb. 2019. "Aerosol Hygroscopic Growth, Contributing Factors, and Impact on Haze Events in a Severely Polluted Region in Northern China." *Atmospheric Chemistry and Physics* 19 (2): 1327–42. https://doi.org/10.5194/acp-19-1327-2019.

315 Chen, Lanxiadi, Chao Peng, Athanasios Nenes, Wenjun Gu, Hanjing Fu, Xing Jian, Huanhuan Zhang, et al. 2020. "On Mineral Dust Aerosol Hygroscopicity." Preprint. Aerosols/Laboratory Studies/Troposphere/Chemistry (chemical composition and reactions). https://doi.org/10.5194/acp-2020-442.

Covert, D. S., R. J. Charlson, and N. C. Ahlquist, 1972: A Study of the Relationship of Chemical Composition and Humidity to Light Scattering by Aerosols. *J. Appl. Meteor. Climatol.*, **11**, 968–976,
320   https://doi.org/10.1175/1520-0450(1972)011<0968:ASOTRO>2.0.CO;2.

Dawson, K. W., R. A. Ferrare, R. H. Moore, M. B. Clayton, T. J. Thorsen, and E. W. Eloranta. 2020. "Ambient Aerosol Hygroscopic Growth From Combined Raman Lidar and HSRL." *Journal of Geophysical Research: Atmospheres* 125 (7): e2019JD031708. https://doi.org/10.1029/2019JD031708.

Dusek, U., G. P. Frank, L. Hildebrandt, J. Curtius, J. Schneider, S. Walter, D. Chand, et al. 2006. "Size Matters More Than
325   Chemistry for Cloud-Nucleating Ability of Aerosol Particles." *Science* 312 (5778): 1375–78. https://doi.org/10.1126/science.1125261.

Düsing, S., Ansmann, A., Baars, H., Corbin, J. C., Denjean, C., Gysel-Beer, M., Müller, T., Poulain, L., Siebert, H., Spindler, G., Tuch, T., Wehner, B., and Wiedensohler, A.: Measurement report: Comparison of airborne, in situ measured, lidar-based, and modeled aerosol optical properties in the central European background – identifying sources of deviations,
330   Atmos. Chem. Phys., 21, 16745–16773, https://doi.org/10.5194/acp-21-16745-2021, 2021.

Feingold, Graham, and Bruce Morley. 2003. "Aerosol Hygroscopic Properties as Measured by Lidar and Comparison with in Situ Measurements." *Journal of Geophysical Research: Atmospheres* 108 (D11): 2002JD002842. https://doi.org/10.1029/2002JD002842.

Fernández, A.J., A. Apituley, I. Veselovskii, A. Suvorina, J. Henzing, M. Pujadas, and B. Artíñano. 2015. "Study of Aerosol
335   Hygroscopic Events over the Cabauw Experimental Site for Atmospheric Research (CESAR) Using the Multi-Wavelength Raman Lidar Caeli." *Atmospheric Environment* 120 (November): 484–98. https://doi.org/10.1016/j.atmosenv.2015.08.079.

Foth, A., H. Baars, P. Di Girolamo, and B. Pospichal. 2015. "Water Vapour Profiles from Raman Lidar Automatically Calibrated by Microwave Radiometer Data during HOPE." *Atmospheric Chemistry and Physics* 15 (14): 7753–63. https://doi.org/10.5194/acp-15-7753-2015.

Gomez, S. L., C. M. Carrico, C. Allen, J. Lam, S. Dabli, A. P. Sullivan, A. C. Aiken, et al. 2018. "Southwestern U.S. Biomass Burning Smoke Hygroscopicity: The Role of Plant Phenology, Chemical Composition, and Combustion Properties." *Journal of Geophysical Research: Atmospheres* 123 (10): 5416–32. https://doi.org/10.1029/2017JD028162.

Granados-Muñoz, M. J., Navas-Guzmán, F., Bravo-Aranda, J. A., Guerrero-Rascado, J. L., Lyamani, H., Valenzuela, A., Titos, G., Fernández-Gálvez, J., and Alados-Arboledas, L.: Hygroscopic growth of atmospheric aerosol particles based on active remote sensing and radiosounding measurements: selected cases in southeastern Spain, Atmos. Meas. Tech., 8, 705–718, https://doi.org/10.5194/amt-8-705-2015, 2015.

Gysel, M., J. Crosier, D. O. Topping, J. D. Whitehead, K. N. Bower, M. J. Cubison, P. I. Williams, M. J. Flynn, G. B. McFiggans, and H. Coe. 2007. "Closure Study between Chemical Composition and Hygroscopic Growth of Aerosol Particles during TORCH2." *Atmospheric Chemistry and Physics* 7 (24): 6131–44. https://doi.org/10.5194/acp-7-6131-2007.

Hänel, Gottfried. 1976. "The Properties of Atmospheric Aerosol Particles as Functions of the Relative Humidity at Thermodynamic Equilibrium with the Surrounding Moist Air." In *Advances in Geophysics*, 19:73–188. Elsevier. https://doi.org/10.1016/S0065-2687(08)60142-9.

Hansen, J., M. Sato, and R. Ruedy. 1997. "Radiative Forcing and Climate Response." *Journal of Geophysical Research: Atmospheres* 102 (D6): 6831–64. https://doi.org/10.1029/96JD03436.

Hu, Qiaoyun. 2018. "Advanced aerosol characterization using sun/sky photometer and multi-wavelength Mie-Raman lidar measurements." (PhD Thesis). Université de Lille, Sciences et Technologies, Lille, France.

Louf, V., Pujol, O., Sauvageot, H., Riédi, J., 2015. Seasonal and diurnal water vapour distribution in the sahelian area from microwave radiometric profiling observations. Quarterly Journal of the Royal Meteorological Society 141, 2643–2653. doi:10.1002/qj.2550

Navas-Guzmán, Francisco, Giovanni Martucci, Martine Collaud Coen, María José Granados-Muñoz, Maxime Hervo, Michael Sicard, and Alexander Haefele. 2019. "Characterization of Aerosol Hygroscopicity Using Raman Lidar Measurements at the EARLINET Station of Payerne." *Atmospheric Chemistry and Physics* 19 (18): 11651–68. https://doi.org/10.5194/acp-19-11651-2019.

Petters, M. D. and Kreidenweis, S. M.: A single parameter representation of hygroscopic growth and cloud condensation nucleus activity, Atmos. Chem. Phys., 7, 1961–1971, https://doi.org/10.5194/acp-7-1961-2007, 2007.

Sicard, M., Fortunato dos Santos Oliveira, D. C., Muñoz-Porcar, C., Gil-Díaz, C., Comerón, A., Rodríguez-Gómez, A., and Dios Otín, F.: Measurement report: Spectral and statistical analysis of aerosol hygroscopic growth from multi-wavelength lidar measurements in Barcelona, Spain, Atmos. Chem. Phys., 22, 7681–7697, https://doi.org/10.5194/acp-22-7681-2022, 2022.

Thorsen, Tyler J., Richard A. Ferrare, Seiji Kato, and David M. Winker. 2020. "Aerosol Direct Radiative Effect Sensitivity Analysis." Journal of Climate 33 (14): 6119–39. https://doi.org/10.1175/JCLI-D-19-0669.1.

Twomey, S., and J. Warner, 1967: Comparison of Measurements of Cloud Droplets and Cloud Nuclei. J. Atmos. Sci., 24, 702–703, https://doi.org/10.1175/1520-0469(1967)024<0702:COMOCD>2.0.CO;2.

Veselovskii, Igor, Qiaoyun Hu, Philippe Goloub, Thierry Podvin, Boris Barchunov, and Mikhail Korenskii. 2022. "Combining Mie–Raman and Fluorescence Observations: A Step Forward in Aerosol Classification with Lidar Technology." *Atmospheric Measurement Techniques* 15 (16): 4881–4900. https://doi.org/10.5194/amt-15-4881-2022.

Veselovskii, Igor, Qiaoyun Hu, Philippe Goloub, Thierry Podvin, Mikhail Korenskiy, Olivier Pujol, Oleg Dubovik, and Anton Lopatin. 2020. "Combined Use of Mie–Raman and Fluorescence Lidar Observations for Improving Aerosol Characterization: Feasibility Experiment." *Atmospheric Measurement Techniques* 13 (12): 6691–6701. https://doi.org/10.5194/amt-13-6691-2020.

Whiteman, D. N., Melfi, S. H., and Ferrare, R. A.: Raman lidar system for the measurement of water vapor and aerosols in the earth's atmosphere, Appl. Opt., 31, 3068–3082, doi:10.1364/AO.31.003068, 1992.

Zieger, P., Aalto, P. P., Aaltonen, V., Äijälä, M., Backman, J., Hong, J., Komppula, M., Krejci, R., Laborde, M., Lampilahti, J., de Leeuw, G., Pfüller, A., Rosati, B., Tesche, M., Tunved, P., Väänänen, R., and Petäjä, T.: Low hygroscopic scattering enhancement of boreal aerosol and the implications for a columnar optical closure study, Atmos. Chem. Phys., 15, 7247–7267, https://doi.org/10.5194/acp-15-7247-2015, 2015